Modifying the Substrate Specificity of Staphylococcal Lipases†

Muriel D. van Kampen, Hubertus M. Verheij, and Maarten R. Egmond*

Department of Enzymology and Protein Engineering, Centre for Biomembranes and Lipid Enzymology, Institute of Biomembranes, Utrecht University, The Netherlands

Received January 15, 1999; Revised Manuscript Received April 1, 1999

ABSTRACT: The lipase from *Staphylococcus hyicus* (SHL) displays a high phospholipase activity whereas the homologous *S. aureus* lipase (SAL) is not active or hardly active on phospholipid substrates. Previously, it has been shown that elements within the region comprising residues 254−358 are essential for the recognition of phospholipids by SHL. To specifically identify the important residues, nine small clusters of SHL were individually replaced by the corresponding SAL sequence within region 254−358. For cloning convenience, a synthetic gene fragment of SHL was assembled, thereby introducing restriction sites into the SHL gene and optimizing the codon usage. All nine chimeras were well-expressed as active enzymes. Eight chimeras showed lipase and phospholipase activities within a factor of 2 comparable to WT-SHL in standard activity assays. Exchange of the polar SHL region 293−300 by the more hydrophobic SAL region resulted in a 32-fold increased k_{cat}/K_m* value for lipase activity and a concomitant 68-fold decrease in k_{cat}/K_m* for phospholipase activity. Both changes are due to effects on catalytic turnover as well as on substrate affinity. Subsequently, six point mutants were generated; G293N, E295F, T297P, K298F, I299V, and L300I. Residue E295 appeared to play a minor role whereas K298 was the major determinant for phospholipase activity. The mutation K298F caused a 60-fold decrease in k_{cat}/K_m* on the phospholipid substrate due to changes in both k_{cat} and K_m*. Substitution of F298 by a lysine in SAL resulted in a 4-fold increase in phospholipase activity. Two additional hydrophobic to polar substitutions further increased the phospholipase activity 23-fold compared to WT-SAL.

Lipases (glycerol ester hydrolase, EC 3.1.1.3) are versatile enzymes that have been isolated from a variety of eukaryotic and prokaryotic organisms. These enzymes have as their primary activity the hydrolysis of neutral lipids such as triglycerides. The active site of lipases contains a catalytic triad consisting of a serine, a histidine, and an acidic residue which in the case of lipases is either an aspartate or a glutamate. This catalytic machinery is covered by an amphipathic surface loop, the so-called 'lid'. Upon interaction of the lipase with an interface, the lid moves away, thus explaining interfacial activation (*1*). Moreover, it has been proposed that the lid region is involved in interfacial interaction and substrate recognition. Lipases have evolved to hydrolyze water-insoluble triglycerides at a lipid−water interface and often show stereo- and regioselectivity. In addition to these natural substrates, they also degrade water-soluble and insoluble esters, Tweens, and rarely phospholipids (reviewed in refs *2*−*4*). One example of a lipase which hydrolyzes phospholipids is the enzyme from guinea pig pancreas. The high phospholipase activity of this enzyme has originally been correlated with the absence of a lid, but studies with coypu pancreatic lipase and the construction of hybrid lipases between the guinea pig enzyme and human pancreatic lipase showed that the exact structural basis for this activity remains to be elucidated (*5*−*7*).

The production of lipases is a general property of staphylococci, and lipase genes have been cloned and sequenced for *S. aureus* strains PS54 and NCTC8530, *S. epidermidis* strains 9 and RP62A, and *S. hyicus* (*8*−*12*). The 40−46 kDa mature parts of these lipases are closely related, suggesting a comparable tertiary structure. All are capable of hydrolyzing triglycerides, but only the enzyme of *S. hyicus* has a high phospholipase activity as well, distinguishing the enzyme from other bacterial lipases (*11*, *13*, *14*). Due to their high homology, the staphylococcal lipases provide an interesting system to study the significance of particular regions and positions for their substrate selectivity. In a recent publication, we reported the construction of chimeras of *S. hyicus* lipase (SHL)[1] and *S. aureus* NCTC8530 lipase (SAL), displaying 53% identity and 64% similarity at the amino acid level (*15*). This study showed that three regions within the C-terminal half of SHL contain elements needed for the recognition of phospholipids. Additionally, the serine following the active site histidine has been identified to be one of the important residues (*16*). In the present study, we wanted to specifically identify the residues within the regions coding for amino acids 254−274 and 275−358 that confer

† This research has been supported by a grant from the EC (Grant BIO2 CT94-3013). The work was carried out under the auspices of the Dutch Foundation for Chemical Research (SON) with financial aid from the Council for Chemical Sciences of The Netherlands Organization for Scientific Research (CW-NWO).

* To whom correspondence should be adressed at P.O. Box 80054, 3508 TB Utrecht, The Netherlands. Phone: +31-30-2533186. Fax: +31-30-2522478. E-mail: maarten.egmond@unilever.com.

[1] Abbreviations: SHL, *Staphylococcus hyicus* lipase; SAL, *Staphylococcus aureus* lipase; PGL, *Pseudomonas glumae* lipase; $pNPC_4$, *p*-nitrophenyl butyrate; C_{16}thioPC, 2-hexadecanoylthioethane-1-phosphocholine; L-diC_8PC, 1,2-dioctanoyl-*sn*-glycero-3-phosphocholine; L-diC_8PG, 1,2-dioctanoyl-*sn*-glycero-3-phosphoglycol.

10.1021/bi990096d CCC: $18.00
Published on Web 06/25/1999

phospholipase activity to SHL. Using this information, we wondered if it would be possible to introduce phospholipase activity into SAL by generating the reverse mutations. To identify the important residues, we wished to replace small fragments of SHL within the regions of interest by the corresponding sequence of SAL and analyze the effect on phospholipase activity of the resulting products. The most convenient cloning procedure for the exchange is cassette mutagenesis, i.e., simple replacement of small restriction fragments with synthetic DNA duplexes containing the desired nucleotide changes. However, the presence of only two unique restriction sites within the region of interest limits the suitability of the WT-SHL gene for this purpose. Previous publications describe the generation of restriction sites in the genes for bovine rhodopsin, thymidylate synthase, and streptavidin by complete synthesis of these genes (*15*−*17*). The synthetic genes were designed, making use of codon degeneracy, to contain a large number of restriction sites evenly distributed throughout the gene sequence. Furthermore, synthetic genes have been constructed to enhance expression by codon optimization (*17*−*19*). Recently, a lipase gene from *Candida rugosa* has been synthesized with a number of unique restriction sites and an optimized nucleotide sequence in terms of heterologous expression in yeast (*20*).

In this paper, we describe the design and construction of a synthetic gene fragment of SHL coding for amino acids 252−366. We used the ligation of overlapping nucleotides as has been described for the synthesis of a tRNA gene as early as 1970 by Khorana and co-workers (reviewed in ref *21*). The lipase from the synthetic SHL gene was expressed, and its characteristics were compared to the native WT-SHL. Additionally, small fragments of the synthetic gene were replaced by the corresponding SAL sequence, and the effect of the replacements on the expressed lipase was studied for phospholipase and lipase activity. Furthermore, the contribution of one fragment was studied in more detail by the generation of point mutants. After specific identification of the involved residues, we were able for the first time to engineer phospholipase activity in SAL.

MATERIALS AND METHODS

Chemicals. Oligonucleotides (reverse-phase cartridge purified) were purchased from Pharmacia. 2-Hexadecanoylthioethane-1-phosphocholine (C_{16}thioPC) was synthesized as described before (*22*). 1,2-Dioctanoyl-*sn*-glycero-3-phosphocholine (L-diC_8PC) and 1,2-dioctanoyl-*sn*-glycero-3-phosphoglycol (L-diC_8PG) were prepared according to standard procedures (*23*). *p*-Nitrophenyl esters were obtained from Sigma. Nickel−nitrilotriacetate was obtained from Invitrogen. All other chemicals were of analytical grade.

DNA Manipulations and Construction of Plasmids. All enzymes for DNA manipulations were purchased from New England Biolabs and applied according to manufacturer's instructions. *E. coli* strain DH5α was used for all plasmid constructions. Mutagenesis was performed using the Quikchange site-directed mutagenesis method according to manufacturer's instructions (Stratagene). The construction of plasmids pMK1 and pMK2, encoding respectively the histidine-tagged mature SHL and SAL, has been described before (*15*). Plasmid pUC18 was digested with *Eco*RI/*Bam*HI and the resulting overhangs were filled in. The plasmid was religated, thereby removing the *Eco*RI, *Kpn*I, *Ava*I, and *Bam*HI sites of the polylinker. The *Xba*I/*Pst*I fragment of pMK1 was cloned into the corresponding sites of this truncated pUC18, resulting in pMK1b. An *Nsi*I site was introduced into the WT-SHL gene of pMK1 by silent mutagenesis of the Leu367 codon using the mutagenic oligonucleotide 5′-GGAAATGATGCATTGGATACAAAACATTC-3′ and its complement. The sites of mutations are underlined. The *Mfe*I/*Pst*I fragment of the mutant gene was sequenced using the dideoxy chain termination method (*24*) and subcloned into the corresponding sites of pMK1b, resulting in plasmid pMK1+N.

The construction of V359S-SAL, plasmid pMK3b, and plasmid 6 (class VII) has been described before (*15*, *16*). Mutagenesis to construct F298K-SAL and AH2-SAL was performed with plasmid V359S-SAL using the respective mutagenic oligonucleotides 5′-CTTAAATATGTTTTTCCCTAAGGTGATTACTGGTAAC-3′ and 5′-GCAGACTTAAATATGGAATTCACCAAAGTGATTACTGGTAAC-3′ and their complements. The *Smi*I/*Pst*I fragment of plasmid pMK3b was replaced by the corresponding fragment of plasmids F298K-SAL and AH2-SAL, resulting in pMK13 and pMK14. The 819 bp *Hin*dIII/*Sca*I fragment of plasmid 6 (class VII), containing the C-terminal SHL sequence T346−A399, was cloned into the *Hin*dIII/*Sca*I sites (partial digest) of F298K-SAL and AH2-SAL, resulting in pMK15 and pMK16.

Construction of Synthetic SHL DNA. The computer program used to identify the possible location of restriction sites was written in Turbo Pascal by M. R. Egmond and is available upon request. The gene fragment coding for Thr252−Ala366 of SHL was assembled from two segments. Use was made of the preferred *E. coli* codons Ala: GCT, Arg: CGT, Asn: AAC, Asp: GAC, Cys: TGC, Gln: CAG, Glu: GAA, Gly: GGT, His: CAC, Ile: ATC, Leu: CTG, Lys: AAA, Phe: TTC, Pro: CCG, Ser: TCT, Thr: ACC, Tyr: TAC, Val: GTT. Each segment was constructed with eight overlapping oligonucleotides as follows. Oligonucleotides F1−F4 and R1−R4 (see Figure 1) were phosphorylated separately and annealed in a 15 μL reaction mixture, consisting of 2.5 pmol of each oligonucleotide in buffer (10 mM Tris−acetate, pH 7.5, 10 mM magnesium acetate, and 50 mM potassium acetate). The annealing mixture was incubated at 90 °C for 10 min and allowed to cool to room temperature over 1 h. Plasmid pMK1+N was digested with *Mlu*I/*Nsi*I, and the vector fragment was purified from gel using QIAEX II gel extraction (Qiagen). The annealed oligonucleotide segment (0.15 pmol) was ligated into *Mlu*I/*Nsi*I-digested pMK1+N vector (0.015 pmol) in a 20 μL reaction volume in ligation buffer. T4 DNA ligase (400 units) was added followed by 2 h incubation at room temperature. A 10 μL portion of the ligation mixture was used to transform *E. coli*. DNA was isolated from several transformants and characterized by restriction analysis, and the sequence of 1−3 isolates was verified by DNA sequencing (*24*). The resulting product was named pMK10. To repair the sequence, the 16 bp *Mfe*I/*Bgl*II fragment of pMK10 was replaced by a DNA cassette of two annealed oligonucleotides, 5′-AATTGGGTAAACACATCGCA-3′ and 5′-GATCTGCGATGTGTTTACCC-3′. Subsequently, the second gene segment was

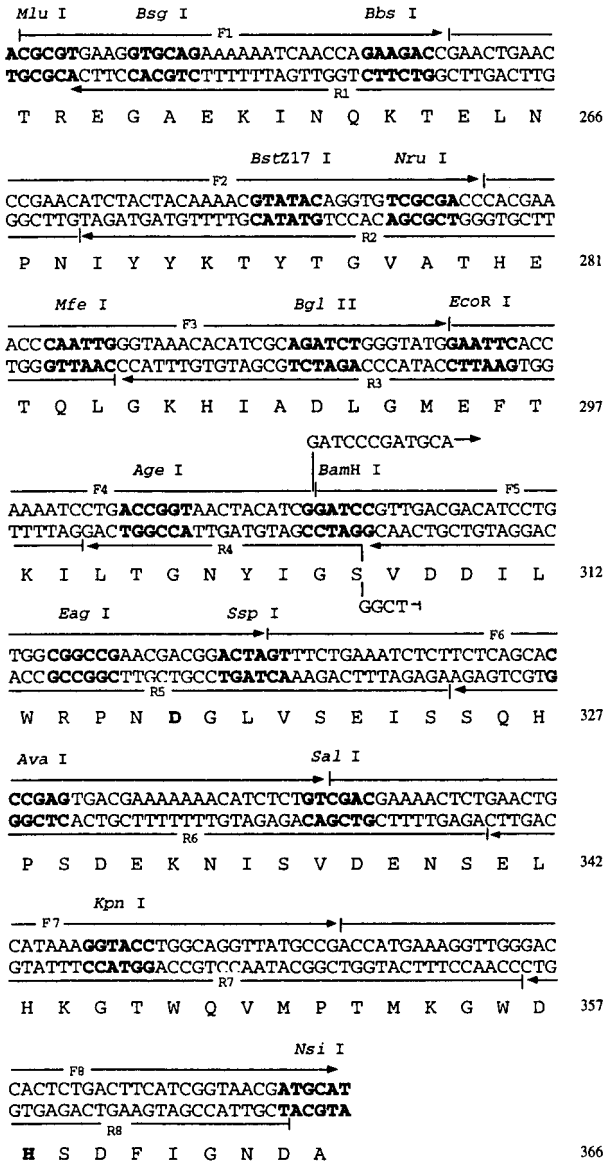

FIGURE 1: Design of a synthetic gene fragment of SHL. The synthetic fragment codes for the region T252−A366. The numbering is given as has been described before (*15*). Individual oligonucleotides (F1−F8 and R1−R8) are indicated by arrows. Unique restriction sites are given in boldface, with the appropriate restriction enzyme listed above the sequence. Active site residues D317 and H358 are given in boldface.

assembled from oligonucleotides F5−F8 and R5−R8 as described above. The segment was cloned into the *Bam*HI/*Nsi*I sites of the repaired pMK10, resulting in plasmid pMK12.

SHL/SAL Exchange. To replace small regions of SHL by SAL sequence, cassette mutagenesis was performed using pMK12 as a starting point. All mutations, cloning sites, and oligonucleotides used are shown in Table 1. HA1−HA5, HA7, and HA8 were constructed by digestion of pMK12 with the appropriate restriction enzymes, purification of the vector fragment from gel, and insertion of a cassette of the two annealed oligonucleotides. For HA6, pMK12 was digested with *Ava*I and *Kpn*I and subsequently treated with Mung bean nuclease to remove the 3′ *Kpn*I and 5′ *Ava*I extensions. After gel purification, the vector fragment was dephosphorylated, and the cassette of two annealed phosphorylated oligonucleotides was inserted.

Small-Scale Expression and Determination of Specific Activities in Cell Lysates. E. coli strain DH5α was freshly transformed with the appropriate chimeric construct. Transformants were used to inoculate overnight cultures in 10 mL of Luria−Bertani medium. Cells were collected by centrifugation and dissolved in 1 mL of application buffer (6 M guanidine hydrochloride, 5 mM imidazole, 10 mM Tris/HCl, pH 8.2). After centrifugation of the lysate (10 min, 16000*g*), 10 μL aliquots of the clear supernatant were taken for activity measurements. Nickel−nitrilotriacetate resin [150 μL of 50% slurry (QIAGEN), equilibrated in application buffer] was added to the remaining supernatant followed by 4 h incubation at 4 °C on a rotating wheel. Subsequently, the resin was washed twice for 15 min at 4 °C with 1 mL of wash buffer (5 mM imidazole, 10 mM Tris/HCl, pH 8.2). The amount of bound lipase was determined by activity measurements of the supernatant. Finally, the protein was eluted by addition of 300 μL of sodium dodecyl sulfate−polyacrylamide gel electrophoresis loading buffer (0.25% bromophenol blue, 0.25% xylene cyanol FF, 30% glycerol) and subsequent boiling of the samples for 3 min. Sodium dodecyl sulfate−polyacrylamide gel electrophoresis (SDS−PAGE) was performed with 5−10 μL aliquots of the protein samples using 15% acrylamide gels with Coomassie brilliant blue staining (*25*). Lipase amounts were determined by scanning densitometry, and these numbers were used to calculate specific activities.

One Liter Scale Expression and Purification. E. coli strain DH5α transformed with the construct was grown on a 1 L scale for 24 h. Cells were collected by centrifugation and dissolved in 75 mL of application buffer. After centrifugation of the lysate (60 min, 16000*g*), the clear supernatant was loaded onto a column of 10 mL of nickel−nitrilotriacetate resin (QIAGEN) equilibrated in application buffer at 4 °C. Subsequently, the resin was washed with 100 mL of application buffer. The lipase was eluted with 500 mM imidazole in application buffer. The eluted lipase was dialyzed for 24 h against 5 mM NaAc, pH 6.0.

Enzymatic Activity Measurements. Spectrophotometric Assays. Activities were determined spectrophotometrically at pH 8.0 (50 mM Tris/HCl) in the presence of 10 mM $CaCl_2$ at room temperature. In standard assays, activity toward *p*-nitrophenyl butyrate ($pNPC_4$) was determined in mixed micelles with Triton X-100 (0.75 mM substrate in 5 mM Triton X-100). The formation of the *p*-nitrophenoxide ion was monitored at 400 nm. Activity on phospholipids was determined in mixed micelles using C_{16}thioPC as a substrate (0.25 mM in 0.2 mM Triton X-100). In the phospholipase assay, 0.2 mM 5,5′-dithiobis(2-nitrobenzoic acid) was included, and the increase in absorption was followed at 412 nm. Activities are given in units (1 unit is the conversion of 1 μmol of substrate per minute) and were calculated using molar extinction coefficients of 16 888 M^{-1} cm^{-1} (*p*-nitrophenoxide) and 13 600 M^{-1} cm^{-1} (2-nitro-5-thiobenzoic acid anion).

Kinetic Analysis. Activities were determined spectrophotometrically essentially as described above. In three-dimensional experiments, activities were measured at varying concentrations of Triton X-100 ranging from 0 to 30 mM and containing a fixed mole percentage of substrate (0.5, 1.0, 2.5, 5.0, and 7.5 mol % of either $pNPC_4$ or C_{16}thioPC). The molar extinction coefficient of the *p*-nitrophenoxide ion

Table 1: Oligonucleotides and Cloning Sites Used for SHL/SAL Exchange[a]

plasmid	mutations	oligonucleotides	cloning sites
HA1	V277E, E281K, T282A, -283L, Q284N, L285S, G286D, K287R, H288Q, I289K	5'-TACCGGTGAAGCTACCCACAAAGCTTTGAACTCTGACCGTCAG-AAAGCA-3' and 5'-GATCTGCTTTCTGACGGTCAGAGTTCAAAGCTT-TGTGGGTAGCTTCACCGGTA-3'	*Bst*Z17 I, *Bgl* II
HA2	G293N, E295F, T297P, K298F, I299V, L300I	5'-GATCTGAACATGTTCTTTCCGTTCGTTATCA-3' and 5'-CCGGTGA-TAACGAACGGAAAGAACATGTTCA-3'	*Bgl* II, *Age* I
HA3	Y304L, S307K, V308A, D309T, D310E, I311K, L312E	5'-CCGGTAACCTGATCGGTAAAGCTACCGAAAAAGAATGGC-3' and 5'-GGCCGCCATTCTTTTTCGGTAGCTTTACCGATCAGGTTA-3'	*Age* I, *Eag* I
HA4	P315E	5'-GATCTGTTGACGACATCCTGTGGCGTGAAAACGACGGA-3' and 5'-CTAGTCCGTCGTTTTCACGCCACAGGATGTCGTCAACA-3'	*Bam*H I, *Spe* I
HA5	E322V	5'-CTAGTTTCTGTTATCTCTAGCCAGCAT3' and 5'-TCGGATGCTGGC-TAGAGATAACAGAAA-3'	*Spe* I, *Ava* I
HA6	S329F, D330N, E331Q, K332A, N333Y, I334T, S335K, V336A, D337T, E338D, N339K, S340-, E341-, L342I, H343Q, (T346I)[a]	5'-CCATTTAACCAAGCTTACACCAAAGCTACCGACAAAATCCAGA-AAGGTAT-3' and 5'-ATACCTTTCTGGATTTTGTCGGTAGCTTTGGTG-TAAGCTTGGTTAAATGG-3'	*Ava* I (nuclease treated), *Kpn* I (nuclease treated)
HA7	M350T, M353K, K354H, G355D	5'-TTGGCAGGTTACCCCGACCAAACACGACTGGGACCACTCTGAC-TTCATCGGTAACGATGCA-3' and 5'-TCGTTACCGATGAAGTCAGAG-TGGTCCCAGTCGTGTTTGGTCGGGGTAACCTGCCAAGTAC-3'	*Kpn* I, *Nsi* I
HA8	E257T, K258D, I259L, Q261R, E264S, Y270V	5'-CGCGTGAAGGTGCAACCGACCTGAACCGTAAGACAAGCTTGAA-CCCGAACATCGTTTACAAAACGTA-3' and 5'-TACGTTTTGTAAACG-ATGTTCGGGTTCAAGCTTGTCTTACGGTTCAGGTCGGTTGCACCTT CA-3'	*Mlu* I, *Bst*Z17 I
HA9	T346I	5'-CTGCATAAAGGTATCTGGCAGGTTATG-3' and 5'-CATAACCTGCCAGATACCTTTATGCAG-3'	
	G293N	5'-GATCTTAACATGGAATTTACCAAAATCCTGA-3' and 5'-CCGGTCAGGATTTTGGTAAATTCCATGTTAA-3'	*Bgl* II, *Age* I
	E295F	5'-GATCTTGGTATGTTCTTTACCAAAATCCTGA-3' and 5'-CCGGTCAGGATTTTGGTAAAGAACATACCAA-3'	*Bgl* II, *Age* I
	T297P	5'-GATCTTGGTATGGAATTTCCGAAAATCCTGA-3' and 5'-CCGGTCAGGATTTTCGGAAATTCCATACCAA-3'	*Bgl* II, *Age* I
	K298F	5'-GATCTTGGTATGGAATTTACCTTCATCCTGA-3' and 5'-CCGGTCAGGATGAAGGTAAATTCCATACCAA-3'	*Bgl* II, *Age* I
	I299V	5'-GATCTTGGTATGGAATTTACCAAAGTACTGA-3' and 5'-CCGGTCAGTACTTTGGTAAATTCCATACCAA-3'	*Bgl* II, *Age* I
	L300I	5'-GATCTTGGTATGGAATTTACCAAAATCATTA-3' and 5'-CCGGTAATGATTTTGGTAAATTCCATACCAA-3'	*Bgl* II, *Age* I

[a] Mutation T346I is not included in the final plasmid.

and the 2-nitro-5-thiobenzoic anion was experimentally determined for different concentrations of Triton X-100 under the assay conditions. The obtained data were fitted according to Michaelis−Menten kinetics. Affinity constants for the micellar interface (K_m) and maximal reaction velocities (V_{max}^{app}) were derived from the fits. The resulting V_{max}^{app} values were plotted as a function of the mole percent of substrate in so-called two-dimensional plots. From the Michaelis−Menten fits of these curves, both the catalytic turnover (k_{cat}) and the interfacial affinity constant (K_m*) values were obtained.

pH-Stat Assays. Activities were measured at 40 °C by titrating released fatty acids with 7.5 mM NaOH under nitrogen. A radiometer titration set consisting of a PHM-84 pH meter, a TTT-80 titrator, an ABU-80 autoburet, a TTT-60 titration assembly, and a Rec-80 servograph was used. Lipase activity was measured on tributyrin in mixed micelles at pH 8.0 (60 mM tributyrin, 120 mM Triton X-100, 5 mM Tris/HCl, 100 mM NaCl, and 10 mM $CaCl_2$). Phospholipase activity was assayed on pure micelles of L-diC_8PC and L-diC_8PG at a concentration of 3 mM in the presence of 50 mM NaCl and 10 mM $CaCl_2$ at pH 8.0 (5 mM Tris/HCl).

RESULTS

Design and Construction of the Synthetic Gene Fragment. Previously, it has been shown that three regions confer phospholipase activity to SHL (*15*). To identify the residues within regions 254−274 and 275−358 that are important for the recognition of phospholipids, we wished to replace small fragments of SHL within these regions by the corresponding SAL sequence. To facilitate cassette mutagenesis, a synthetic gene fragment was designed, incorporating unique restriction sites throughout the SHL sequence of interest. For the start of this fragment, the *Mlu*I site, already present in the WT sequence at the Thr252 codon, could be used. Introduction of an *Nsi*I site at the Ala366 codon made it possible to replace the DNA region coding for Thr252−Ala366 by a synthetic counterpart. The DNA sequence was based on the amino acid sequence of SHL (*9*) and was designed using the following strategy. A computer program identified the possible location of restriction sites making use of the codon degeneracy. Only those sites were selected which were not located in the remaining part of SHL and/or in the cloning vector pUC18 (except in the polylinker region). Furthermore, the codons that were not included in restriction sites were modified to those that are preferentially used in highly expressed *E. coli* genes (*26*). Following this strategy, a 77 nucleotide change could accomplish the optimization of 46 codons and the introduction of 12 unique restriction sites (2 restriction sites were maintained) between the *Mlu*I and the *Nsi*I sites.

For construction of the synthetic gene fragment, pMK1 (his-tagged WT-SHL in pUC18) was used as a cloning vector. Prior to gene assembly, four sites were deleted from the polylinker region, and an *Nsi*I site was introduced into the WT-SHL gene by site-directed mutagenesis. The synthetic fragment was assembled from two gene segments. Each segment was composed of 8 overlapping oligonucleotides ranging from 26 to 52 nucleotides in length, which code for both strands of the gene (see Figure 1). The first segment consisted of the *Mlu*I/*Bam*HI sequence. Downstream of the *Bam*HI site, a short sequence compatible with *Nsi*I

was added to clone the segment immediately into the *Mlu*I/*Nsi*I sites of pMK1. After ligation and transformation, plasmid DNA was isolated from several transformants and characterized by restriction analysis. Sequencing of three isolates, containing the appropriate restriction pattern, showed a 4 bp deletion (GTAA) between the *Mfe*I and *Bgl*II sites in all three clones. This deletion could easily be repaired by cassette mutagenesis, inserting a synthetic DNA duplex of the correct sequence between the *Mfe*I and *Bgl*II sites. To obtain the complete gene, the second segment consisting of the *Bam*HI/*Nsi*I sequence was assembled from eight oligonucleotides and cloned into the corresponding sites of the repaired plasmid. Restriction analysis of DNA isolates showed the absence of a *Sal*I site in two of four sequences, whereas all other introduced sites were present. The two other isolates contained all introduced sites. Sequencing of one of the latter isolates yielded the correct sequence. The new plasmid was named pMK12. Expression on a 10 mL scale revealed that the production of lipase/cell density was about 2-fold higher as compared to pMK1 (not shown).

SHL/SAL Exchange. Plasmid pMK12 was used as the starting point to replace small regions of SHL by the corresponding SAL sequence. Initially, we wanted to replace eight regions, ranging from 1 to 16 mutations per replacement. The appropriate amino acid changes for plasmids HA1−HA8 are indicated in Table 1. Here the amino acid numbering refers to the numbering as introduced before (*15*). Cloning of all plasmids succeeded except for HA6. Construction of this plasmid yielded several clones which contained the first 15 mutations, but lacked the T346I mutation. Most likely, Mung bean nuclease did not remove the 3′ *Kpn*I extension, in which the codon for T346 is located. Treatment with a 10-fold excess of Mung bean nuclease did not yield the proper result either. Only 1 sequence was obtained which showed all 16 amino acid mutations, but contained an additional insertion coding for 6 amino acids (HLTKLT) between I346 and W347, resulting in HA6-ins. Therefore, the T346I mutation was made separately by site-directed mutagenesis (HA9). Small-scale expression of the lipase from the plasmids and SDS−PAGE showed that the cells produced 200−1000 μg of lipase/10 mL of overnight culture. To test if the chimeric lipases were enzymatically active, the activity in the lysate of cells expressing the enzyme was determined toward *p*-nitrophenyl butyrate (0.75 mM $pNPC_4$ in 5 mM Triton X-100). Subsequently, the determination of phospholipase activity was performed by a spectrophotometric assay using C_{16}thioPC as a substrate, on which SHL displays a high phospholipase activity, while SAL does not. Specific activities were calculated on the basis of the measured activity and the estimates of the amounts of lipase determined by SDS−PAGE (see Materials and Methods).

Inspection of the data in Table 2 shows that the specific activities of WT-SHL (pMK1) on both $pNPC_4$ and C_{16}thioPC were 2-fold lower as compared to the activities of the synthetic variant (pMK12). Nevertheless, the relative activities were identical. Also, all chimeras displayed a high activity on $pNPC_4$, indicating that these are properly folded enzymes. Furthermore, the specific activities on $pNPC_4$ of all chimeras were comparable to that of the parent pMK12, except for HA2 and HA7, which respectively showed a 7-fold increase and a 2-fold decrease (Table 2). Interestingly, the chimera with the six amino acid insertion (HA6-ins) also shows a specific activity similar to pMK12, indicating that the enzyme has some conformational freedom within that part of the structure (data not shown). Phospholipase/lipase ratios were calculated and are shown in Table 2. Clearly, only HA2 shows a decrease in this ratio of 200-fold, whereas all other chimeras display ratios comparable to the parent pMK12. The exchanged region of HA2, comprising residues 293−300, contains six amino acid differences between SHL and SAL: G293N, E295F, T297P, K298F, I299V, and L300I. To examine the contribution of each individual residue to phospholipase activity, six point mutants were made by cassette mutagenesis starting from pMK12. Both pMK12, HA2 and the point mutants were expressed on a 1 L scale and purified by affinity chromatography in one step to about 90% purity in yields of 7-30 mg. Activities were measured on both $pNPC_4$ and C_{16}thioPC. Specific activities and phospholipase/lipase ratios of the pure lipases were calculated, and the results are shown in Table 3. In agreement with the activities measured in cell lysates (Table 2), the pure HA2 displays an increase in $pNPC_4$ acivity, whereas the activity on C_{16}thioPC is markedly decreased. Inspection of the data for the point mutants shows that the mutations G293N, T297P, I299V, and L300I have only minor influences on the phospholipase/lipase ratio. On the contrary, E295F and K298F display a reduction in this ratio of respectively 2.5- and 32-fold, due to both an increase in lipase activity and a decrease in phospholipase activity. These results indicate that within region 274−358, K298 is the major determinant for phospholipase activity, whereas E295 plays a minor role. In addition, lipase activity was tested on the true triglyceride substrate tributyrin (Table 3). Only HA2 showed a clear increase in specific activity on this substrate relative to WT-SHL.

Table 2: Enzymatic Activities and Phospholipase/Lipase Ratios of the SHL/SAL Chimeras in Cell Lysates[a]

plasmid (exchanged region)	$pNPC_4$ (units/mg)	C_{16}thioPC (units/mg)	C_{16}thioPC/$pNPC_4$
pMK1	110	194	1.8
pMK12	237	415	1.8
HA1 (277−289)	252	429	1.7
HA2 (293−300)	1512	13	0.009
HA3 (304−312)	203	374	1.8
HA4 (315)	280	372	1.3
HA5 (322)	195	349	1.8
HA6 (329−343)	204	406	2.0
HA7 (350−355)	98	142	1.5
HA8 (257−270)	249	356	1.4
HA9 (346)	276	341	1.6

[a] Activities given are average values of duplicate measurements. The range of duplicate values was within 25% (specific activities) and 10% (phospholipase/lipase ratio).

Subsequently, we wanted to investigate the kinetic basis for the changes in both lipase and phospholipase activity for the SHL variants HA2, E295F, and K298F. The activity of lipolytic enzymes at a micellar interface can be divided into two steps according to the model as proposed by Verger and De Haas (*27*). The first step involves the binding of the enzyme to the interface, resulting in an interfacially bound enzyme form, E*. This step is followed by the binding of substrate into the active site of E*, whereupon the catalytic steps can take place. First, so-called three-dimensional experiments were performed in mixed micelles composed of varying concentrations of Triton X-100 with a fixed mole

Table 3: Enzymatic Activities of Pure WT-SHL, HA2, and SHL Point Mutants[a]

	$pNPC_4$ (units/mg)	C_{16}thioPC (units/mg)	C_{16}thioPC/$pNPC_4$	tributyrin (units/mg)	L-diC_8PC (units/mg)	L-diC_8PG (units/mg)	PC/PG
pMK1	252	349	1.38	307	643	237	2.8
pMK12	401	505	1.27	545	917	333	2.8
HA2	2273	19	0.008	2500	46	42	1.1
G293N	287	437	1.55	384	705	261	2.7
E295F	623	315	0.51	397	264	58	4.6
T297P	451	555	1.41	357	476	126	3.8
K298F	880	35	0.04	553	58	13	4.5
I299V	223	346	1.59	220	417	158	2.6
L300I	302	530	1.75	364	598	136	4.4

[a] Activities given are average values of duplicate measurements. The range of duplicate values was within 10%.

Table 4: Kinetic Analysis of WT-SHL, HA2, and SHL Point Mutants on Lipase Activity[a]

	K_m* (mol % $pNPC_4$)	k_{cat} (s^{-1})	k_{cat}/K_m* [s^{-1} (mol %)$^{-1}$]
WT (pMK12)	5.5 ± 2.0	397 ± 77	73
HA2	1.3 ± 0.2	3000 ± 172	2308
E295F	2.2 ± 0.6	366 ± 35	167
T297P	2.7 ± 1.1	206 ± 34	76
K298F	5.7 ± 2.3	927 ± 201	163

[a] Activities were measured in mixed micelles of Triton X-100 and $pNPC_4$ as a substrate. Deviations given are as calculated from the Michaelis−Menten fits.

Table 5: Kinetic Analysis of WT-SHL, HA2, and SHL Point Mutants on Phospholipase Activity[a]

	K_m* (mol % C_{16}thioPC)	k_{cat} (s^{-1})	k_{cat}/K_m* [s^{-1} (mol %)$^{-1}$]
WT (pMK12)	6.3 ± 1.1	315 ± 23	50
HA2	23 ± 4	17.3 ± 2.1	0.74
E295F	7.4 ± 0.9	165 ± 9	22
T297P	6.9 ± 2.1	419 ± 59	61
K298F	57 ± 5	47.6 ± 3.6	0.84

[a] Activities were measured in mixed micelles of Triton X-100 and C_{16}thioPC as a substrate. Deviations given are as calculated from the Michaelis−Menten fits.

percentage of $pNPC_4$. Curves were collected for five different mole percentages of $pNPC_4$ for the three variants, WT-SHL (pMK12) and T297P. The latter point mutant displayed comparable characteristics as WT-SHL in the standard assays (Table 3). The obtained saturation curves were fitted according to Michaelis−Menten kinetics, and the affinity for the micellar interface (K_m) and the maximal reaction velocity (V_{max}^{app}) were determined at each mole percentage of $pNPC_4$. The point mutants E295F, T297P, and K298F showed K_m values comparable to WT (3.3 ± 0.9 mM Triton X-100), whereas HA2 displayed a slightly lower affinity (K_m of 10 ± 3 mM Triton X-100). The obtained V_{max} values were plotted as a function of the mole percentage of $pNPC_4$ in two-dimensional plots, and again saturation curves were obtained. From the fitted data, both the catalytic turnover constant (k_{cat}) and the interfacial affinity constant (K_m*) were derived. The ratio k_{cat}/K_m* was calculated, and the results are shown in Table 4. Interestingly, the high lipase activity of HA2 is caused by both a decrease in K_m* and an increase in k_{cat} resulting in a 32-fold higher k_{cat}/K_m* ratio compared to WT-SHL. For E295F, T297P, and K298F, only minor changes were observed in both parameters. In agreement with the specific activities in the standard assay (Table 2), E295F and K298F showed a slightly higher lipase activity relative to WT-SHL as evidenced by the 2-fold increase in k_{cat}/K_m*. Then, kinetic constants regarding phospholipase activity were determined. For all enzymes including WT-SHL, the affinity for the mixed micellar interface was higher with K_m values below 1 mM Triton X-100. Saturation curves were obtained after plotting the V_{max} values versus the mole percentage of C_{16}thioPC. The obtained kinetic parameters derived from the Michaelis-Menten fits are shown in Table 5. Obviously, the decrease in phospholipase activity of HA2 and K298F is due to effects on catalytic turnover as well as substrate affinity, resulting in a 60−70-fold decrease in the k_{cat}/K_m* value for either variant. For E295F, the 2-fold decrease in k_{cat}/K_m* is caused by a decrease in k_{cat} rather than an increase in K_m*.

Subsequently, we wanted to study the effect of the mutations on phospholipid headgroup specificity. To this end, activities were determined on pure micelles of phospholipids with either a zwitterionic headgroup (L-diC_8PC) or a negatively charged headgroup (L-diC_8PG). Specific activities and PC/PG ratios are shown in Table 3. In agreement with the measurements on C_{16}thioPC, both HA2 and K298F display a large reduction in specific activity on the phospholipid substrates. On the other hand, influences on the PC/PG ratio, reflecting the preference for either headgroup, are small for all mutants. For HA2, a comparable activity is found for either a PC or a PG headgroup. Just like pMK12, G293N and I299V show a small preference for the zwitterionic choline group to the negatively charged phosphoglycol group. This phenomenon is somewhat more pronounced for E295F, T297P, K298F, and L300I.

SAL Mutants. Based on the observations noted above for SHL variants, we wondered if it would be possible to introduce phospholipase activity into SAL by exchanging the identified amino acids in SAL for the corresponding SHL residues. Since Ser359, located next to the active site His in SHL, has already been identified to play a role in phospholipid recognition (*16*), the V359S mutant of SAL was used as the starting point for these mutations. First, the mutation F298K was made by site-directed mutagenesis. Furthermore, the effect of the three simultaneous mutations F295E, P297T, and F298K (AH2-SAL), replacing three hydrophobic residues by three polar ones, was studied. The three mutants and WT-SAL (pMK2) as a control were expressed on a 1 L scale and purified by affinity chromatography to about 90% purity in final yields of 60 mg. Specific activities and phospholipase/lipase ratios are listed in Table 6. The SAL mutants display a reduced activity on $pNPC_4$ compared to WT-SAL. Nevertheless, the phospholipase activity has increased by a factor 4 for the mutation F298K, and a 23-

Table 6: Enzymatic Activities of Pure WT-SAL, SAL Point Mutants, and Chimeras[a,b]

	$pNPC_4$ (units/mg)	C_{16}thioPC (units/mg)	C_{16}thioPC/ $pNPC_4$	L-diC_8^{PC} (units/mg)
pMK2	132	0.045	0.00034	0.031
SAL-V359S	77	0.02	0.00026	nd
SAL-F298K[c]	15	0.16	0.011	0.066
SAL-AH2[c]	39	1.02	0.026	0.35
pMK13	8.4	0.11	0.013	0.20
pMK14	29	1.31	0.045	0.43
pMK15	6.2	0.47	0.076	0.092
pMK16	11	2.01	0.18	—[d]

[a] Activities given are average values of duplicate measurements. The range of duplicate values was within 10%. [b] nd: not determined. [c] The V359S mutation is included in this mutant. [d] not detectable (200 μg in test).

fold increase has been accomplished by the introduction of the three polar residues. Recently, it has been shown that apart from the difference in phospholipase activities, SAL and SHL are quite different in chain length selectivity with SAL being mainly active on short-chain substrates (*13*). Furthermore, it has been shown that elements within region G180−R253 of SHL provide the main contribution to the hydrolysis of long acyl chains (*15*). First, taking this difference into account, we also tested the activity of the SAL mutants with the shorter chain L-diC_8PC as a substrate (Table 6). Nevertheless, no activity improvement was seen compared to C_{16}thioPC. Additionally, in an attempt to improve the phospholipase activity of the SAL mutants on the long-chain C_{16}thioPC, the central SHL region 180−254 was introduced into both F298K-SAL and AH2-SAL, resulting in pMK13 and pMK14, respectively. Since the C-terminal residues (region 359−399) also contribute to phospholipase activity (*16*), pMK15 and pMK16 were constructed in which residues I346−A399 of F298K-SAL and AH2-SAL were replaced by the corresponding residues of SHL. The chimeric enzymes were expressed and purified in yields of 30−60 mg (pMK13 and pMK14) and 7−8 mg (pMK15 and pMK16). Characteristics of the resulting chimeras are given in Table 6. While for all chimeras, $pNPC_4$ activities were reduced up to 20-fold, the phospholipase/lipase ratios increased to a maximum value of 530-fold for pMK16 compared to WT-SAL (pMK2).

DISCUSSION

The two staphylococcal lipases which were used in this study are homologous proteins showing 53% identity and 64% similarity at the amino acid level. The N-terminal halves of these proteins display a higher percentage of conserved residues than the C-terminal portions (respectively 59 and 48% identity). In general, conserved residues in enzymes are involved in catalysis and generation of the correct three-dimensional structure, i.e., in formation of disulfide bridges, salt bridges, and residues in the core of the proteins. Variable positions are often found in loops on the surface of enzymes and in regions near the substrate binding site. Thus, analysis of such variable residues can provide information about the structural basis of substrate specificity (*28*, *29*). Usually, specificity is determined by several residues which assemble in the tertiary structure. Consequently, the use of random mutagenesis techniques is limited by the amount of clones and the number of mutations per clone which have to be screened to identify all the important residues. For staphylococcal lipases, no X-ray structure is available, and sequence homology with other lipase families is too low for computer-based modeling of the complete structure. Hence, it was also not possible to use a directed approach for structure−function analysis of these enzymes. Therefore, we have first identified regions within the primary sequence of SHL that are essential for the recognition of phospholipids by the generation of SHL/SAL chimeric enzymes (*15*).

In SHL, three regions have been identified containing residues important for the high phospholipase activity of the enzyme (*15*). These regions are all located in the C-terminal half of the protein (residues 254−399). In this paper, we show the replacement of high variability clusters of SHL in region 254−358 by the corresponding sequence of SAL, which is not active on phospholipids. For cloning convenience, a synthetic gene of the SHL region of interest was generated, thereby introducing unique restriction sites throughout the sequence. Additionally, the codon usage within this region was successfully optimized, resulting in a 2-fold higher expression of the lipase. First, nine regions comprising 1−15 amino acid differences were exchanged between SHL and SAL. Replacement of the complete region 254−274 (HA8) only resulted in a minor decrease in the phospholipase/lipase ratio. Thus, this region does not seem to play an essential role in phospholipid hydrolysis, in contrast with earlier findings obtained with SAL/SHL chimeric enzymes (*15*). However, these latter chimeras all contained the N-terminal half of SAL, including residues involved in the oxyanion hole and the active site serine that are important for substrate hydrolysis as well. Further analysis of the phospholipase activities of the chimeras containing replacements in the region 275−358 shows that a high phospholipase activity is determined by the region comprising amino acids 293−300. If any, only minor effects were observed for replacement of the other high-variability clusters within the region 275−358. The fact that in all cases the lipase activity is more or less comparable to WT-SHL demonstrates the tolerance of the lipase toward such replacements. Moreover, even in the presence of a six amino acid insertion between I346 and W347, the lipase is still highly active. Probably, this region is located at the surface of the lipase where it can join in the formation of a loop, without affecting the integrity of the protein scaffold. The fact that WT-SAL contains two deletions at positions 340 and 341 underscores the notion that this part of the lipase has some conformational freedom.

The most likely explanation for the phospholipase activity of SHL is an evolution of one of the subsites, i.e., the binding pockets for *sn*-1 or *sn*-2 chains of the substrate, from an apolar site to a more polar site capable of interacting with the phospholipid headgroup. In SHL, this site is still able to bind an acyl chain as well. Replacement of region 293−300 involves six mutations, of which two are conservative replacements (I299V and L300I), three are mutations from a polar to a more hydrophobic residue (E295F, T297P, and K298F) and the remaining mutation is G293N. Interestingly, a 6-fold increase in lipase activity as compared to WT-SHL has been generated by the exchange of region 293−300 (HA2), indicating the importance of hydrophobic residues within this region for a high lipase activity. On the other hand, since a 27-fold decrease in phospholipase activity is introduced simultaneously, the presence of polar residues is

likely to determine the ability to degrade phospholipids. Obviously, these results indicate that region 293−300 is involved in formation of the binding pocket for the *sn*-1 or *sn*-2 chain of the substrate. Since no X-ray structure of the staphylococcal lipases is available, we used sequence alignment to evaluate the position of this region in the X-ray structure of the lipase from *Pseudomonas glumae* (PGL) (*30*). Recently, Simons and co-workers published a sequence alignment of the staphylococcal lipases and PGL (*31*). It was shown that several secondary structure elements as predicted for the staphylococcal lipases are quite similar to those observed in the structure of PGL. Furthermore, it was clear that the homology is especially high for the regions surrounding the active site residues and for residues 1−117 (PGL numbering) of the lipases. From the PGL structure, it can readily be seen that this N-terminal part together with the C-terminal α-helix comprises most of the core of the lipase, i.e., the α/*β*-hydrolase fold. The majority of the loops and helices in the C-terminal half of the lipase is located at the surface surrounding the active site entrance and may thus be involved in substrate recognition. Although amino acids 293−300 were present in a region of low homology, these residues were aligned with region 243−250 of PGL. This region forms an α-helix in PGL (α9), which is located near the active site entrance. Interestingly, in the X-ray structure of *Pseudomonas cepacia* lipase (84% identity with PGL), complexed with a triglyceride analogue, A246 and T250 interact with the *sn*-1 chain of the inhibitor (*32*). This result supports our finding that the corresponding region 293−300 in SHL may well be involved in formation of the substrate binding pocket.

The generation of six point mutants in region 293−300 shows that K298F substantially reduces the phospholipase/lipase ratio in standard assays, whereas a small decrease in this ratio is found for E295F. The other four point mutants (G293N, T297P, I299V, and L300I) show ratios comparable to WT-SHL (pMK12). A kinetic analysis was performed to investigate the basis for the changes in both lipase and phospholipase activity of HA2 (region 293−300 replaced), E295F, and K298F. The results were compared to the kinetic parameters of WT-SHL and T297P, the latter displaying the same k_{cat}/K_m* values as WT-SHL in both assays. HA2 displays a 32-fold increase in the k_{cat}/K_m* value for lipase activity, whereas the increase for the point mutants E295F and K298F is only 2-fold for each. Thus, the high lipase activity of HA2 must likely be ascribed to the combination of mutations rather than one individual point mutation. Concerning phospholipase activity, the largest differences are found for HA2 and K298F, displaying respectively a 68-fold and a 60-fold decrease in k_{cat}/K_m* value relative to WT-SHL. Both changes are due to a catalytic turnover as well as a substrate affinity effect. The results indicate that K298 is the major determinant for the high phospholipase activity of SHL, while E295 plays a minor role. Indeed as has been elaborated above, two polar residues seem to be involved in the recognition of phospholipids. In terms of substrate binding, the positively charged lysine may interact with the negatively charged phosphate oxygen. A possible role for E295 might be the formation of a salt bridge with K298 to maintain the correct position of the lysine residue. This possibility suggests an α-helical character of this region in the lipase structure.

Previously, it has been shown for porcine pancreatic phospholipase A_2 that substitution of a lysine for a methionine in the substrate headgroup binding pocket improved the activity on zwitterionic substrates and reduced the activity on negatively charged substrates (*33*). Analyzing the phospholipid headgroup specificity of the six SHL point mutants revealed only small effects on the preference for either a glycol or a choline headgroup compared to WT-SHL. This finding suggests that the mutated residues are probably not involved in direct interactions with the glycol or choline group.

After identification of the important residues in SHL, we were able to introduce phospholipase activity into SAL by generating the reverse mutations. The F298K mutation in combination with the previously described V359S mutation caused both a 4-fold increase in phospholipase activity and a 32-fold increase in phospholipase/lipase ratio compared to SAL-WT. However, the 5-fold decrease in lipase activity might indicate a destabilizing effect of the positively charged lysine. Interestingly, this effect is decreased upon the simultaneous replacement of three hydrophobic residues by three polar ones, F295E, P297T, and F298K, in V359S-SAL. This finding could indicate the formation of a stabilizing salt bridge between E295 and K298 as has been suggested above. Even more interestingly, a 23-fold increase in phospholipase activity and a 72-fold increase in ratio were accomplished by the four simultaneous mutations. Thus, the introduction of polarity in the presumed headgroup binding region seems to be as important as the presence of an individual lysine at position 298 for the absolute specific activity of the enzyme. Subsequently, a set of four chimeras was generated by replacing larger regions of the SAL mutants by the corresponding SHL sequence. Introduction of either the central SHL region 180−254 or the C-terminal region 346−399 reduced the $pNPC_4$ activity even further by a factor of 2−3 compared to the parent mutants. On the other hand, the phospholipase/lipase ratio for the chimeras increased to a maximum value of 530-fold compared to SAL-WT.

In conclusion, the use of a synthetic gene is a convenient tool to facilitate cassette mutagenesis in order to study structure/function relationships of proteins. We showed that region 295−298 of SHL probably interacts with the phospholipid substrate, in which K298 is the major determinant. Most likely, this region is involved in formation of the substrate binding site. In SHL, introduction of hydrophobic residues in this presumed binding site resulted in a very high lipase activity and a lower phospholipase activity. Notably, we were for the first time able to introduce phospholipase activity into SAL by replacement of three hydrophobic residues for polar residues within this region.

ACKNOWLEDGMENT

We thank Mr. Ruud Cox and Mr. Ruud Dijkman for synthesis of the substrates.

REFERENCES

1. Rubin, B. (1994) *Struct. Biol. 1*, 568−572.
2. Derewenda, Z. S. (1994) *Adv. Protein Chem. 45*, 1−52.
3. Ransac, S., Carrière, F., Rogalska, E., Marguet, F., Buono, G., Pinho Melo, E., Cabral, J. M. S., Egloff, M.-P., Van

Tilbeurgh, H., and Cambillau, C. (1996) in *Engineering of/with lipases*, pp 143−182, Kluwer, London.
4. Jaeger, K.-E., Ransac, S., Dijkstra, B. W., Colson, C., Van Heuvel, M., and Misset, O. (1994) *FEMS Microbiol. Rev. 15*, 29−63.
5. Hjorth, A., Carrière, F., Cudrey, C., Wöldike, H., Boel, E., Lawson, D. M., Ferrato, F., Cambillau, C., Dodson, G. G., Thim, L., and Verger, R. (1993) *Biochemistry 32*, 4702−4707.
6. Carrière, F., Thirstrup, K., Hjorth, S., Ferrato, F., Nielsen, P. F., Withers-Martinez, C., Cambillau, C., Boel, E., Thim, L., and Verger, R. (1997) *Biochemistry 36*, 239−248.
7. Thirstrup, K., Verger, R., and Carrière, F. (1994) *Biochemistry 33*, 2748−2756.
8. Farrel, A. M., Foster, T. J., and Holland, K. T. (1993) *J. Gen. Microbiol. 139*, 267−277.
9. Götz, F., Popp, F., Korn, E., and Schleifer, K. H. (1985) *Nucleic Acids Res. 13*, 5895−5906.
10. Nikoleit, K., Rosenstein, R., Verheij, H. M., and Götz, F. (1995) *Eur. J. Biochem. 228*, 732−738.
11. Simons, J.-W. F. A., Van Kampen, M. D., Riel, S., Götz, F., Egmond, M. R., and Verheij, H. M. (1998) *Eur. J. Biochem. 253*, 675−683.
12. Lee, C. Y., and Iandolo, J. J. (1986) *J. Bacteriol. 166*, 385−391.
13. Simons, J.-W. F. A., Adams, H., Cox, R. C., Dekker, N., Götz, F., Slotboom, A. J., and Verheij, H. M. (1996) *Eur. J. Biochem. 242*, 760−769.
14. Van Oort, M. G., Deveer, A. M. T. J., Dijkman, R., Leuveling Tjeenk, M., Verheij, H. M., De Haas, G. H., Wenzig, E., and Götz, F. (1989) *Biochemistry 28*, 9278−9285.
15. Van Kampen, M. D., Dekker, N., Egmond, M. R., and Verheij, H. M. (1998) *Biochemistry 37*, 3459−3466.
16. Van Kampen, M. D., Simons, J.-W. F. A., Dekker, N., Egmond, M. R., and Verheij, H. M. (1998) *Chem. Phys. Lipids 93*, 39−45.
17. Guillemette, J. G., Matsushima-Hibiya, Y., Atkinson, T., and Smith, M. (1991) *Protein Eng. 4*, 585−592.
18. Holler, T. P., Foltin, S. K., Ye, Q.-Z., and Hupe, D. J. (1993) *Gene 136*, 323−328.
19. Perlak, F. J., Fuchs, R. L., Dean, D. A., McPherson, S. L., and Fischhoff, D. A. (1991) *Proc. Natl. Acad. Sci. U.S.A. 88*, 3324−3328.
20. Brocca, S., Schmidt-Dannert, C., Lotti, M., Alberghina, L., and Schmid, R. D. (1998) *Protein Sci. 7*, 1415−1422.
21. Khorana, H. G. (1979) *Science 203*, 614−625.
22. Aarsman, A. J., Van Deenen, L. L. M., and Van den Bosch, H. (1976) *Bioorg. Chem. 5*, 241−253.
23. Franken, P. A., Van den Berg, L., Huang, J., Gunyuzlu, P., Lugtigheid, R. B., Verheij, H. M., and De Haas, G. H. (1992) *Eur. J. Biochem. 203*, 89−98.
24. Sanger, F., Nicklen, S., and Coulson, A. R. (1977) *Proc. Natl. Acad. Sci. U.S.A. 74*, 5463−5467.
25. Sambrook, J., Fritsch, E. F., and Maniatis, T. (1989) in *Molecular cloning: a laboratory manual* (Ford, N., Nolan, C., and Ferguson, M., Eds.), 2nd ed., Cold Spring Harbor Laboratory Press, Cold Spring Harbor, NY.
26. Grosjean, H., and Fiers, W. (1982) *Gene 18*, 199−209.
27. Verger, R., and De Haas, G. H. (1976) *Annu. Rev. Biophys. Bioeng. 5*, 77−117.
28. Cygler, M., Schrag, J. D., Sussman, J. L., Harel, M., Silman, I., Gentry, M. K., and Doctor, B. P. (1993) *Protein Sci. 2*, 366−382.
29. Lotti, M., Tramontano, A., Longhi, S., Fusetti, F., Brocca, S., Pizzi, E., and Alberghina, L. (1994) *Protein Eng. 7*, 531−535.
30. Noble, M. E. M., Cleasby, A., Johnson, L. N., Egmond, M. R., and Frenken, L. G. J. (1993) *FEBS Lett. 331*, 123−128.
31. Simons, J.-W. F. A., Van Kampen, M. D., Ubarretxena-Belandia, I., Cox, R. C., Alves dos Santos, C. M., Egmond, M. R., and Verheij, H. M. (1999) *Biochemistry 38*, 2−10.
32. Lang, D. A., Mannesse, M. L. M., De Haas, G. H., Verheij, H. M., and Dijkstra, B. W. (1998) *Eur. J. Biochem. 254*, 333−340.
33. Beiboer, S. H. W., Franken, P. A., Cox, R. C., and Verheij, H. M. (1995) *Eur. J. Biochem. 231*, 747−753.

BI990096D